Electronic Supplementary Material (ESI) for Dalton Transactions.

Supporting Information for:

Redox Effects of Low-Spin Ru (II/III) on Slow Magnetic Relaxation of Ru-Mn (III) 1D Cyanide-Bridged Complexes

Xiaoquan Zhu, Shaodong Su, Wenhai Cao, Yuehong Wen, Shengmin Hu, Xintao Wu and Tianlu Sheng*

Table S1. Bond lengths (Å) and angles (deg.) for compound **1**

Ru(1)-C(2)	2.013(3)	C(2)-Ru(1)-C(1)	175.06(15)
Ru(1)-C(1)	2.032(3)	C(2)-Ru(1)-N(9)	92.79(13)
Ru(1)-N(9)	2.104(3)	C(1)-Ru(1)-N(9)	91.74(13)
Ru(1)-N(7)	2.107(3)	C(2)-Ru(1)-N(7)	88.21(14)
Ru(1)-N(5)	2.116(3)	C(1)-Ru(1)-N(7)	89.95(14)
Ru(1)-N(3)	2.131(3)	N(9)-Ru(1)-N(7)	88.54(12)
Mn(1)-O(1)	1.872(3)	C(2)-Ru(1)-N(5)	86.67(13)
Mn(1)-O(2)	1.880(3)	C(1)-Ru(1)-N(5)	88.73(13)
Mn(1)-N(12)	1.974(4)	N(9)-Ru(1)-N(5)	178.11(13)
Mn(1)-N(11)	2.008(4)	N(7)-Ru(1)-N(5)	89.64(12)
Mn(1)-N(2)	2.223(3)	C(2)-Ru(1)-N(3)	90.97(14)
Mn(1)-N(1)	2.229(3)	C(1)-Ru(1)-N(3)	91.09(14)
N(1)-C(1)	1.154(5)	N(9)-Ru(1)-N(3)	88.67(12)
N(2)-C(2)	1.156(5)	N(7)-Ru(1)-N(3)	177.05(12)
		N(5)-Ru(1)-N(3)	93.15(12)
		O(1)-Mn(1)-O(2)	93.38(14)
		O(1)-Mn(1)-N(12)	174.27(16)
		O(2)-Mn(1)-N(12)	91.81(14)
		O(1)-Mn(1)-N(11)	92.82(14)
		O(2)-Mn(1)-N(11)	173.43(14)
		N(12)-Mn(1)-N(11)	81.91(15)
		O(1)-Mn(1)-N(2)	89.15(14)
		O(2)-Mn(1)-N(2)	93.73(12)
		N(12)-Mn(1)-N(2)	88.08(13)
		N(11)-Mn(1)-N(2)	84.15(13)
		O(1)-Mn(1)-N(1)	92.29(13)
		O(2)-Mn(1)-N(1)	95.54(12)
		N(12)-Mn(1)-N(1)	89.64(13)
		N(11)-Mn(1)-N(1)	86.41(12)
		N(2)-Mn(1)-N(1)	170.51(13)
		C(1)-N(1)-Mn(1)	161.3(3)
		C(2)-N(2)-Mn(1)	165.7(3)
		N(1)-C(1)-Ru(1)	177.4(3)
		N(2)-C(2)-Ru(1)	173.6(4)

Table S2. Bond lengths (Å) and angles (deg.) for compound **2**

Ru(1)-C(1)	2.070(13)	C(1)-Ru(1)-N(3)	88.1(5)
Ru(2)-C(2)	2.051(16)	C(1)-Ru(1)-N(5)	88.2(5)
Ru(1)-N(3)	2.098(12)	N(3)-Ru(1)-N(5)	86.8(5)
Ru(1)-N(5)	2.101(12)	C(2)-Ru(2)-N(7)	90.1(5)
Ru(2)-N(7)	2.068(12)	C(2)-Ru(2)-N(9)	90.2(6)
Ru(2)-N(9)	2.093(12)	N(7)-Ru(2)-N(9)	85.9(5)
Mn(1)-O(2)	1.872(11)	O(2)-Mn(1)-O(1)	93.5(5)
Mn(1)-O(1)	1.890(10)	O(2)-Mn(1)-N(11)	172.6(5)
Mn(1)-N(11)	1.979(13)	O(2)-Mn(1)-N(12)	90.7(5)
Mn(1)-N(12)	2.010(13)	O(2)-Mn(1)-N(2)	102.0(5)
Mn(1)-N(1)	2.295(13)	O(2)-Mn(1)-N(1)	90.8(5)
Mn(1)-N(2)	2.344(16)	O(1)-Mn(1)-N(12)	175.4(5)
N(1)-C(1)	1.154(17)	O(1)-Mn(1)-N(11)	93.0(5)
N(2)-C(2)	1.187(19)	O(1)-Mn(1)-N(1)	89.0(5)
		O(1)-Mn(1)-N(2)	88.3(5)
		N(11)-Mn(1)-N(12)	82.9(5)
		N(11)-Mn(1)-N(1)	85.8(5)
		N(11)-Mn(1)-N(2)	81.7(5)
		N(12)-Mn(1)-N(1)	92.7(5)
		N(12)-Mn(1)-N(2)	89.1(5)
		N(1)-Mn(1)-N(2)	167.1(5)
		C(1)-N(1)-Mn(1)	164.9(12)
		C(2)-N(2)-Mn(1)	161.3(13)
		N(1)-C(1)-Ru(1)	177.2(13)
		N(2)-C(2)-Ru(2)	174.1(14)

Table S3. Selected parameters obtained by fitting out-of-phase AC magnetic susceptibility (χ'') vs frequency (ν) plots of complex **2** using Debye model.

T/K	τ / ms	$\tau_{\text{std. dev.}}$ / ms	α	$\alpha_{\text{std. dev.}}$
1.9	0.0285	0.0003	0.141	0.005
2.0	0.0199	0.0003	0.114	0.006
2.1	0.0147	0.0003	0.0915	0.006
2.2	0.0116	0.0004	0.0711	0.007
2.3	0.00904	0.0003	0.0720	0.006
2.4	0.00809	0.0006	0.0634	0.009
2.5	0.00688	0.0005	0.0894	0.010

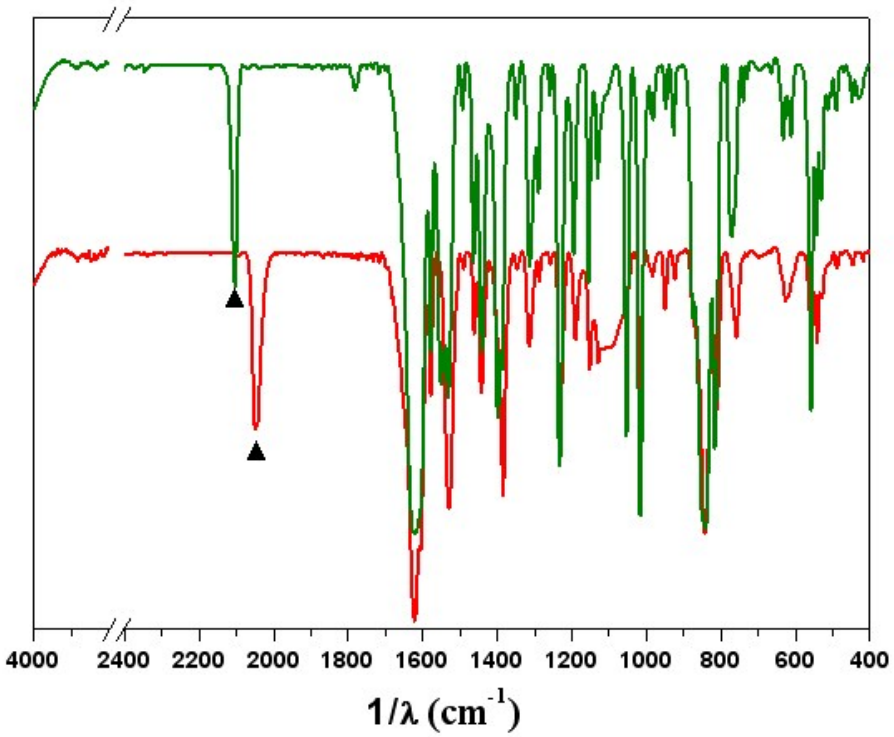

Figure S1. IR spectrum of **1** (red) and **2** (green). The absorption peak at 2049 cm^{-1} is attributed to the stretching vibration of C≡N bonding with Ru^{II}, and the absorption peak at 2103 cm^{-1} is attributed to the stretching vibration of C≡N bonding with Ru^{III}.

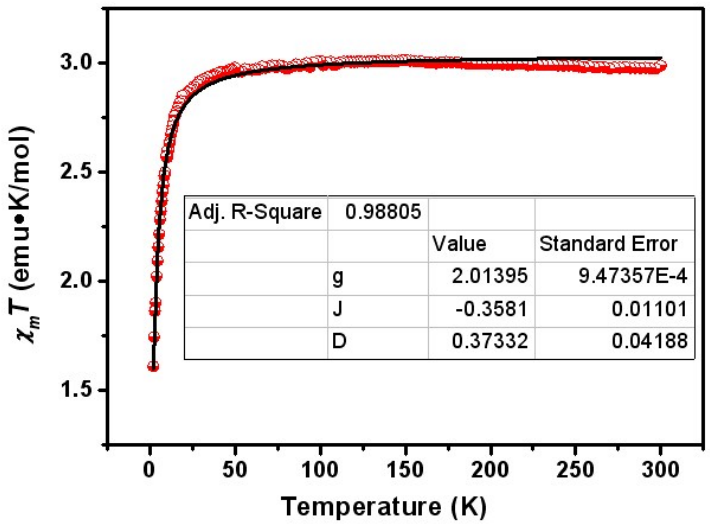

Figure S2. Variable-temperature dc magnetic susceptibility data for **1** (red) and its best-fit result (solid line) using the Fisher model extended by Smith and Friedberg[1]:

$$\chi^* = \frac{Ng^2\beta^2 S(S+1)}{3kT} * \frac{1+u}{1-u}$$

$$(u = \coth[\frac{JS(S+1)}{kT}] - [\frac{kT}{JS(S+1)}]);$$

$$\Delta\chi = \chi_z - \chi_x = \frac{2Ng^2\beta^2 S(S+1)}{15kT} * \frac{DS(S+1)}{kT} F$$

$$(F = \frac{(1+u)(1+v)}{(1-u)(1-v)} + \frac{2u}{1-u}, v = 1 - \frac{3ukT}{JS(S+1)});$$

$$\chi = \frac{2\chi_x + \chi_z}{3} = \frac{\Delta\chi + 3\chi^*}{3}$$

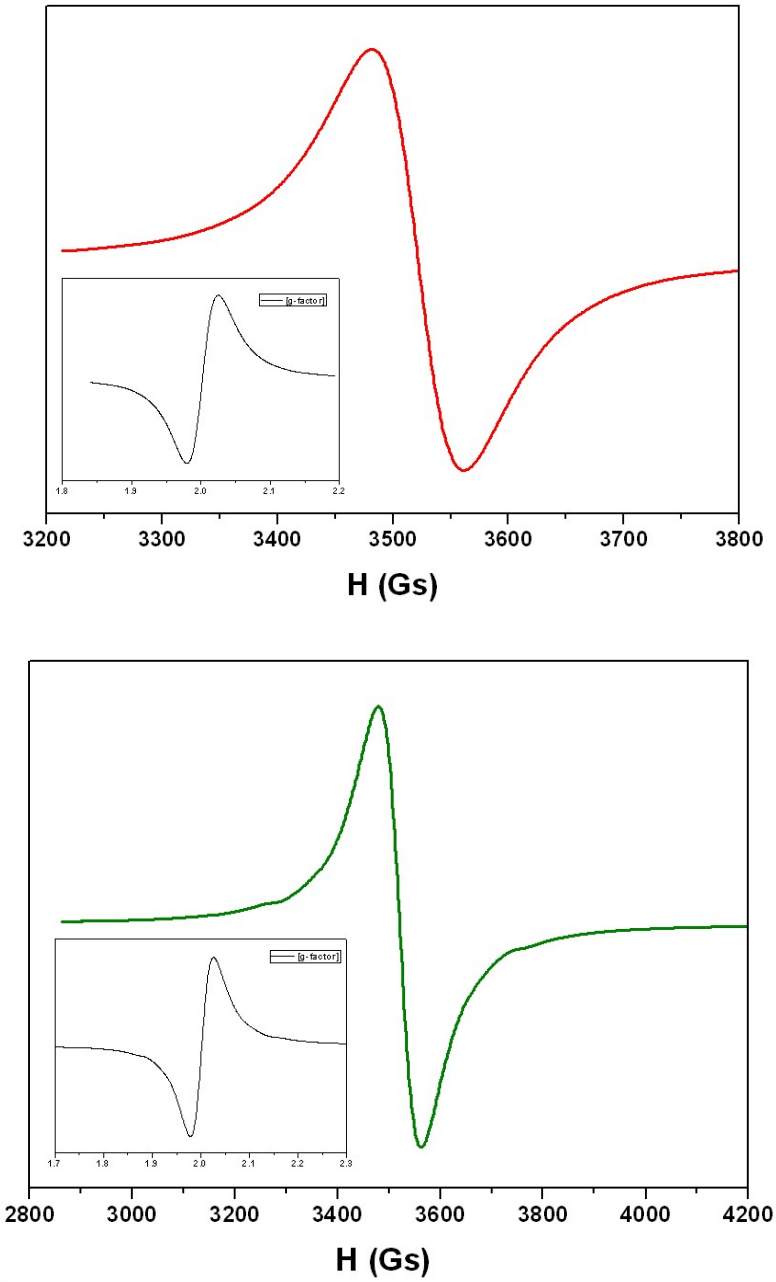

Figure S3. EPR spectra of **1** (top) and **2** (bottom) recorded at room temperature (inset: the g factor).

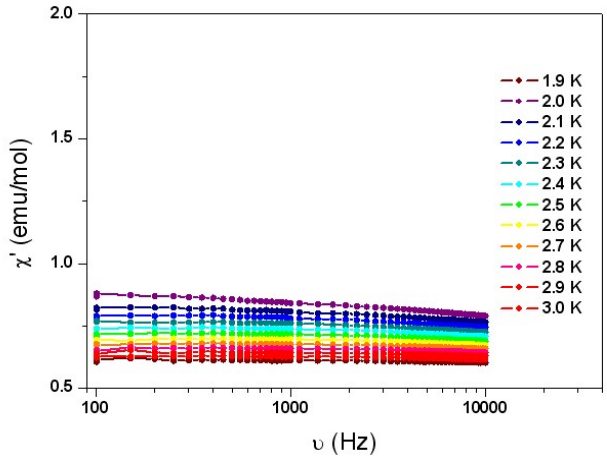

Figure S4. In-phase AC magnetic susceptibility vs frequency data under zero DC field for complex **1**.

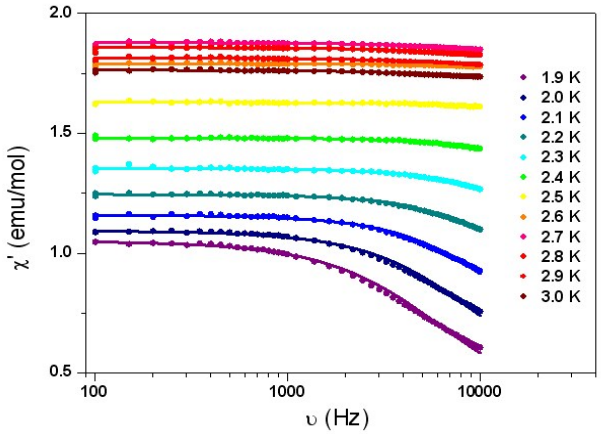

Figure S5. In-phase AC magnetic susceptibility vs frequency data under zero DC field for complex **2**. (solid lines are the best fits to the Debye model.)

REFERENCES

1 Kahn O., *Molecular magnetism*. VCH Publishers, Inc.(USA), 1993, p.257.